LA-UR- 09-00337

Approved for public release;
distribution is unlimited.

Title:	Review: engineering particles using the aerosol-through-plasma method
Author(s):	Jonathan Phillips, Claudia C Luhrs, Monique Richard
Intended for:	IEEE Transactions on Plasmas

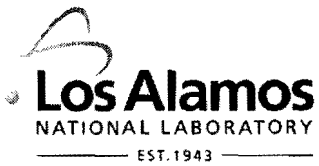

Form 836 (7/06)

Review: Engineering Particles Using the Aerosol-Though-Plasma Method

By Jonathan Phillips [1,2]*, Claudia C. Luhrs [2] and Monique Richard [3]

[1] MST Division, Los Alamos National Lab, Los Alamos, New Mexico 87545

[2] Department of Mechanical Engineering, University of New Mexico, Albuquerque, New Mexico 87103

[3] Toyota Research Institute of North America, 1555 Woodridge, Ann Arbor, MI, 8105

ABSTRACT

For decades plasma processing of materials on the nano-scale has been an underlying enabling technology for many 'planar' technologies, particularly virtually every aspect of modern electronics from integrated circuit fabrication with nano-scale elements to the newest generation of photovoltaics. However, it is only recent developments that suggest plasma processing can be used to make 'particulate' structures of value in fields including catalysis, drug delivery, imaging, higher energy density batteries and other forms of energy storage. In this review the development of the science and technology of one class of plasma production of particulates, Aerosol-Through-Plasma (A-T-P) is reviewed. Various plasma systems, particularly RF and microwave, have been used create nanoparticles of metals and ceramics, as well as supported metal catalysts. Gradually the complexity of the nanoparticles, and concomitantly their potential value, has increased. First, unique two layer particles were generated. These were post-processed to create unique three layer nano-scale particles. Also, the technique has been successfully employed to make other high value materials including carbon nanotubes, unsupported graphene, and spherical boron nitride. Some interesting plasma science has also emerged from efforts to characterize and map aerosol containing plasmas. For example, it is clear that even a very low concentration of particles dramatically changes plasma characteristics. Some have also argued that the local-thermodynamic-equilibrium approach is inappropriate to these systems. Instead, it has been suggested that charged species and neutral species models must be independently developed and allowed to 'interact' only in generation terms.

* to whom correspondence should be addressed

INTRODUCTION

Plasma processing is employed for a remarkable diversity of commercial materials. Clearly the most widespread use, and the one with the greatest economic impact, is the use of plasma 'etching' and thin film deposition in the creation of modern integrated circuits[1,2] . In fact, there is a long history of plasma deposition of films in virtually every aspect of electronic materials including transistors, resistors, capacitors , VLSI, displays, solar cells, etc.[3,4]. Other economically significant applications include the creation of surface coatings with unique properties[5], and the use of plasmas to improve/modify properties of polymer films, particularly adhesion, and for medical application, sterility[6,7]. Recently reviewed[8] and of particular relevance to the present work are commercial applications, primarily surface modification, of atmospheric pressure plasmas. There is one area of atmospheric plasma application, not covered in that review: plasma particle production. Perhaps this reflects the fact that commercial applications of plasma created particulate materials are still 'emerging'.

The present paper reviews plasma production of particulate materials, with an emphasis on the use of one particular technique: Aerosol-Through-Plasma (A-T-P). In this technique, precursors, which can be particles, liquids or even gases, are carried through a plasma region generally at, or near, atmospheric pressure. In the plasma region the precursors are transformed by the very high temperature/unique chemistry encountered. In most cases the residence time in the plasma region is very short, generally only a fraction of a second, yet unique processes take place in that short time because of two features of these plasmas: the extreme temperature (>3500 C), and the wide range of gas composition (e.g. exclusion of oxygen) that can be employed. The new

particulate materials created in the high temperature region of the plasma next enter a chimney where very rapid cooling takes place. Finally, the particulates are captured downstream, generally on filter paper.

Particulate materials of potential commercial importance created using the A-T-P method to date include nano-metal particles, micron sized metal particles of controlled size, nano-oxide particles, core-shell nanoparticles, spherical ceramic particles of controlled size, carbon nanotubes, spherical boron nitride, nano-oxides with two and even three cations, supported metal catalysts, carbon-graphite coated metal particles, hollow micron scale particles and graphene. More recently the products of this technique have been 'post-processed' to create unique, complex structures, such as tri-layer nanoparticles.

A-T-P GENERATION OF PARTICULATE MATERIALS

The primary intent of this essay is to demonstrate that the A-T-P method is a practical means to take advantage of the unique plasma environment for generating particulate materials of commercial value. In an effort to most effectively illustrate the present and near future utility of A-T-P for making valuable 'particles', much of the essay is divided into material categories. A secondary objective is to explain the unique environment of the plasmas most frequently used in the A-T-P method. For this reason, the essay concludes with a section regarding the structure, both as determined experimentally and simulated, of microwave generated atmospheric plasmas.

Simple Nano-Particles

A proposed component of the 'nano' revolution in materials is the generation and application of nanoparticles, for which many applications have been proposed, some of the most recent and promising are for data storage, inks, and bio-imaging applications [9.10,11]. Given the interest in generating a wide variety of nanoparticles it is not surprising to find that there are numerous novel methods under development for the generation of nanoparticles including metal gas evaporation[12,13] metal evaporation in a flowing gas stream[14,15] mechanical attrition [16], ssputtering [17], electron beam evaporation [18], electron beam induced atomization of binary metal azides [19], expansion of metal vapor in a supersonic free jet [20], inverse micelle techniques [21], laser ablation[22], laser-induced breakdown of organometallic compounds[23], and pyrolysis of organometallic compounds[24].

Consistent with the emphasis on' nano', the earliest demonstrations of A-T-P technology were for the generation of nano particles. Even in the earliest work two advantages to the A-T-P method were demonstrated. First, 'reduced state' nanoparticles can be produced. Second, multi-species nano structures can be created. That is, since the process often 'atomizes' the precursors, the atoms from different precursors can recombine to form the final particles.

The alternative methods have limitations that may impact the areas of use of A-T-P synthesis of nanoparticles. Although a thorough analysis is not possible in this format, it is interesting to reflect on the limits of alternative aerosol approaches. Flame synthesis [25,26], is intrinsically limited as oxygen must be present. Even in the best controlled

synthesis, a significant fraction of the particles are oxidized[27]. Moreover, in order to produce partially reduced particles, the precursors are generally dissolved in liquids, requiring that most of the energy input is employed in evaporation, clearly reducing the postulated 'energy efficiency' advantage of the flame synthesis method. More conventional aerosol synthesis of nanoparticles also requires the evaporation of liquid in order to leave a solid residue[28,29,30]. Moreover, neither technique can reach temperatures even approaching those found in plasmas.

MacKinnon et al.[31,32] were among the first to clearly use an 'A-T-P' system to prepare nanoparticles. The system contained many of the same elements found in all the early systems: high power RF, argon 'plasma gas', and gaseous precursor species (Figure 1). An RF power of 28 kW was employed, and the desired product was nanoparticles of boron carbide. The feed gases were boron trichloride, methane and argon. The use of similar, atmospheric pressure, high power RF systems continued for some time. For example, about a decade later a group at Los Alamos National Lab used a similar, better cooled and sturdier system to generate SiC nano particles from gases (silane, methane and hydrogen).

Other groups created more complex plasma systems to generate nanoceramic particles. Yoshida et al. [34] employed a complex 'hybrid' device, using both DC and RF power. The objective was to convert two gas precursors into 'ultra fine' silicon nitride powder. As shown in Figure 2, a plasma jet, containing the gas precursor $SiCl_4$ in Ar, is generated with a DC power supply (ca. 5 kW) and that jet, with shield gas, is fed immediately to a section powered by an RF coil (4 Mhz, > 10 kW). The second reactive gas, NH_3, is fed into the afterglow. The complexity of the device reflected the authors

analysis of the fluid mechanics of plasma systems. They were persuaded by mathematical models, that only a device of this level of complexity would provide sufficient stability for particle production. (It is notable, given later discussion, that the plasma model they employed is a 'local thermodynamic equilibrium' (LTE) model. More recent work suggests this model does not adequately address the differences in temperature between charged and neutral species. See 'Characterization and Modeling' section below.) The powder generated was both nano (30-50 nm) and amorphous. A weak XRD spectra (not shown) of Si_3N_4 was only observed after annealing, and presumably sintering, at over 1800 K.

The first use of a simple microwave system is described by Chou and Phillips [35]. Low power (200W) was used to create nanoparticles of iron, iron oxide and core shell particles, consisting of a core of iron and a shell of carbon. Particles were created from a precursor 'aerosol' stream of ferrocene vapor and a carrier gas (argon, oxygen or hydrogen). Mossbauer spectroscopy (MES) was used to determine the particle phase and transmission electron microscopy (TEM) the size distribution. The impact of two operating parameters was studied: injection point (upstream vs. downstream of the microwave coupler) and gas identity (oxygen, hydrogen or argon) (It is interesting to note that only a microwave system permits the use of a wide variety of gases at low power.). Other operating parameters such as power (200W) and total gas flow rate were kept constant. It was found that metallic iron formed in plasmas containing primarily hydrogen, and that iron oxide particles formed in dominantly oxygen or argon plasmas. Particle size and production rates were strongly influenced by the injection point. The

smallest particles were formed via injection into the afterglow. MES clearly showed the particles made in primarily hydrogen plasmas were zero valent, but size and phase were difficult to determine because the MES spectra were fully 'relaxed' and the core/shell structure made TEM measurements problematic. The particles produced with hydrogen plasmas passed through the coupler were clearly larger, yielding unrelaxed MES spectra characteristic of 'larger' metallic iron (MES) particles, and readily measured using TEM (average diameter between 30 and 60 nm). It was also found that the production rate of nanoparticles was nearly an order of magnitude larger when the aerosol was sent through the entire plasma.

The use of molecular precursors to create nanoparticles continues. For example, Brenner et al[36] generated monometallic iron and cobalt particles and bimetallic CoMo particles from molecular carbonyl precursors (e.g $Fe(CO)_5$). A low pressure (60 torr) microwave system similar to that employed by Chou and Phillips [35] was used and precursor injection was always upstream of the plasma. They found that the particles generated by passage of 'aerosols' containing the carbonyl had a log normal distribution and a particle size less than 10 nm in all cases. There is some 'complexity' to the method as in all cases the metal is encapsulated by or supported by carbon structures. Still, they argue that the technique creates metallic nanoparticles as small or smaller than those produced using any other method (Figure 3).

The first use of non-molecular precursors employed a high power RF plasma (ca. 10 kW). Nano particles were generated by injecting micron sized iron particles through an atmospheric pressure, argon plasma. The afterglow 'chimney' was cooled using gas, and particles collected in a filter [37]. The iron particles (phase not determined), generated

using this method, appear to be spherical in shape. One feature reported repeatedly in later work is the influence of precursor flow rate. At the lowest flow rate employed, average particle radius was about 20 nm, but increased with flow rate. Indeed, increasing the iron particle concentration in the flow by a factor of about four, caused nearly a 15 fold increase in average particle volume.

In other early work high power (>10 kW) DC discharge was used to generate nanoparticles from gases injected downstream from the discharge region[38]. Silicon nanoparticles (ca. 10 nm) were generated from silicon chloride (heated and purged) gas, carbon from methane and silicon carbide from co-injection of those two gases. An effort to model the distribution based on the assumption of complete atomization of the precursor species and population balance approach was not entirely successful [38,39]. For example, the model suggests a log normal distribution should be seen once the average particle reaches about 2 nm, whereas for carbon a monotonic decrease in concentration with increasing particle size was seen even in distributions in which the average particle size was clearly larger than 10 nm. This was one of the first indications of the possibility that nano particle formation in A-T-P systems may involve some unique mechanisms. Still, it is noteworthy that the proposed mechanism is unique to aerosol methods.

The particle size distribution observed in a later study of nano-aluminum metal formation from micron metal particles in a microwave generated plasma (Figure 4) provided additional evidence of the need to reconsider the mechanism of nanoparticle formation during A-T-P [40]. The classic model of nucleation and agglomeration/growth by collision predicts log normal growth, and log normal distributions were not always observed[4142]. Alternatively, models based on Ostwald Ripening, or even multiple

mechanisms, suggest a distribution with a sharp cut-off at a maximum size [43]. Once again, the 'mature' particle size distribution of nano-aluminum particles fit neither model. Consideration was given to the role surface charge might play in particle growth [44] as well as viscous drag. Indeed, in a microwave system, due to the far higher mobility of the electrons, all surfaces charge to a negative potential [45]. Still, careful consideration suggested the effect of added repulsion and viscous drag on particle growth via agglomeration mechanisms would be minimal.

Other aspects of nano-aluminum formation suggest unique capabilities for the A-T-P method. For example, in some operating conditions particles with 'tails' formed (Figure 5). It was suggested that in this case, liquid metal 'broke out' during rapid freezing, leaving hollow particle heads. The generation of oxide particles, rather than metal particles, requires only a slight variation on the A-T-P method required to make metal particles. Specifically, the addition of a small amount of oxygen (<5%) to the same flow stream that produced nano aluminum particles, results in the formation of nano aluminum oxide. Surprisingly, changes in operating parameters influence not only the size of the particles, but the phase of the oxide that forms [46].

At this point in time, technology has advanced to the point that many of the techniques are sufficiently developed for commercialization. Indeed, new companies are forming and selling 'simple' nanoparticles generated using plasma technologies. Research work is now focused on creating more complex structures using plasma technology.

Complex Nano-particles- The recent focus on nanotechnology brings with it the requirement of creating structures, including particle structures, of increasing complexity

at the nanoscale. Much of the new work in 'complex nanoparticles' is application driven. For example, two layer shells, an inner shell of noble metal and an outer shell of silica, were developed for use in medical diagnostics [47]. There are developing applications for the hollow nano metal shells (sans silica) alone, particularly drug delivery strategies[48]. For example, there are numerous methods available to create hollow carbon particles on the nanoscale[49,50,51]. Other applications are in catalysis. Multi-layer, multi-functional, nano-scale 'supports' are in development [52].

One of the best examples of the use of the A-T-P system to create complex nanoparticles is the production of nano-particles with a core of one ceramic, ceria, and a shell of different oxide, alumina [53]. This structure (Figure 6) potentially has value as an 'oxygen buffering' (ceria), but sinter resistant (alumina) support for 3-way catalytic converters [54,55]. It is notable that flame synthesis has been employed to make similar core-shell ceramic nanoparticles [56].

Particles were generated with a simple atmospheric pressure, low power (<1 kW) microwave A-T-P system. Two gas streams flowed through the system (Figure 7). An outer gas (generally argon) is on the 'outside,' and a gas containing the aerosolized powder (generally a mixture of argon and oxygen) is carried to the center of the coupler in a small bore (3mm ID) alumina tube. The inner stream in some circumstances has a 'jet' structure.

Many precursor materials were tried, but the one that yielded particles consistently of the same structure, and at relatively high rates, was generated from a powder produced by evaporating all the liquid from a solution containing nitrates of cerium and aluminum. A key to the formation of the core/shell morphology was postulated to be the preferential

migration of the smaller cation to the surface during oxidation. This process is consistent with known oxidation kinetics. Indeed, iron oxidizes via the diffusion of iron cations, not diffusion of oxygen in any form[57]. The net result is the formation of a core of ceria and a shell of alumina.

One surprising finding in this work was the existence of a dramatic bi-modal particle size distribution. In volumetric terms, it was generally found that micron particles (log normal distribution, average size approximately 1000 nm) and nano particles (log normal distribution, average size about 30 nm) were present in similar quantity. Closer observation revealed that the larger particles were generally hollow (Figure 6). It was also found that some operating condition produced only micron scale particles. In these instances, no hollow particles were observed. It was clear all the particles were solid.

A novel hypothesis was advanced to explain all the data: In the A-T-P production of nanoceramic particles 'shattering' of large, (micron scale) hollow particles creates nano-fragments. The larger hollow 'parent' particles form when clusters of precursor material in the aerosol are suddenly heated in the plasma zone to extreme temperature. This results in the decomposition of the salt complex, or heating of the absorbed solvent , and concomitantly the release of hot volatile gas. This expanding gas pushes a shell of material outward, until it finds a means to escape (e.g. a hole). If the gas escapes 'successfully' a hollow particle forms. If the gas finds no avenue of escape, the expanding 'solid' shell grows until it reaches the level of stress at which it breaks. At this point the internal pressure causes the bubble to burst/ explode/shatter, and concomitantly create nano particles. The application of this model to nanoparticle production in other A-T-P processes (above) is not clear. All the evidence (e.g. the absence of bimodal

distributions in most cases) appears to be consistent with the notion that multiple mechanisms are at work. The dominant mechanism is probably a function of many factors, including the vaporization temperature of the precursors. In the case of metals such as tin and aluminum with low vaporization temperatures, atomization followed by nucleation probably dominates. For high melting temperature species, such as ceramics, the shattering mechanism may generally be more important.

The relatively low surface area (ca. 25 m^2/gm) of the ceria-alumina core/shell particle led workers to try other compositions capable of acting as 'oxygen buffering' and sinter resistant nanoparticles for 3-way catalyst supports[52,58,59]. It was found that titania core/alumina surface particles could be produced with essentially the same technique use to produce ceria core/alumina shell nanoparticles. In contrast to ceria/alumina, these particles were found to be unimodal and of quite high surface area. It was also found that they were unusually stable at high temperatures (Figure 8). Indeed, they were far more stable than particles of identical composition, and initially higher surface area, generated with a standard sol-gel process. The characteristic responsible for the better thermal stability of the A-T-P generated particles is unclear but one hypothesis is: i) particles are formed at the high temperatures found in the torch they are better crystallized than (amorphous) particles formed via a sol gel synthesis, and ii) a higher degree of crystallization imparts greater thermal stability.

Another example of 'complex' nanoparticle formation is the creation of core metal/shell carbon-graphite particles (Figure 9). Particles of this type can be produced using the microwave A-T-P apparatus with solid metal precursor particles, and a variety of gas (ethylene), liquid (hexane) or solid (anthracene) precursors as the source of carbon.

~~Insert figure of metal/carbon structure to show that product is same independent of C-precursor.~~

The core/shell carbon-grahite/metal particles have been used as 'templates' for other particles. For example, it has been shown that a third layer of either silica or alumina can be deposited on core metal/shell carbon-graphite particles using post plasma processing, such as incipient wetness (Figure 10).

This most recent work suggests that the creation of truly unique, 'designer', nanoparticles will likely require the use of a variety of techniques. This parallels the need for multiple steps for the generation of complex circuitry. And it is clear, A-T-P has a place as one tool in the technology of complex particle fabrication.

Multiscale Materials: Supported Metal Catalysts

In this review, supported metal catalysts are treated as a distinct class of A-T-P generated material. They are not 'complex nanoparticles', but actually 'multiscale' materials. Although one component, the 'active' metal, is generally on the nanoscale, the other component, 'inert support' is generally not on the nanoscale. This multiscale arrangement achieves low cost by dispersing the active and expensive phase (e.g. platinum, palladium, rhodium) in small particles, yet allows low pressure drop with a non-nanoscale inexpensive phase (e.g. alumina). This arrangement also prevents, to a degree, aging by agglomeration of the active phase by 'locking' the metal to the support.

A simple atmospheric pressure microwave system was employed for the first A-T-P generated supported metal catalyst[60,61]. In this process the precursor consisted of metal salts and some precursor materials, in relative amounts consistent with that generally

found for commercial catalysts (ca. 1% by weight metal). The dry powder, a simple physical mixture, was sent through an argon plasma, and the product collected on filter paper downstream. This early work demonstrated that the A-T-P method can be employed to create highly dispersed, active, supported metal catalysts.

The apparent advantage of the process was the relative simplicity of fabrication: assemble components by physical mixing, generate an aerosol, pass through a plasma (<1 second) and collect catalyst. This eliminated many long slow steps associated with 'incipient wetness' the least expensive and most common process for generating supported metal catalysts, including: i) 'wet' impregnation, ii) high temperature calcining and iii) reduction.

Experiments have been performed to determine if ATP produced catalysts that are compositionally, and apparently morphologically, identical to catalysts created using conventional approaches, have the same properties as conventional catalyst. For example, carbon supported Pd and PdAg catalysts were employed as catalysts for selectively hydrogenating acetylene in a stream of primarily ethylene. This is a test not so much a test of catalyst activity, but is more a test of selectivity. A-T-P generated PdAg/Carbon catalysts (Figure 11) showed superior selectivity to the commercial PdAg/Alumina catalysts [62].

Additionally, there are numerous studies of catalyst 'modification' in plasmas. In these studies the catalyst, or pre-catalyst, is exposed to a plasma environment at some point after metal is already dispersed in some fashion on a ceramic or carbon support. For example, one group used a low pressure (~1 torr) hydrogen plasma generated with RF to replace the normal post incipient wetness calcinations step to prepare 1% Pd/alumina [63].

That is, the metal salts were already dried and dispersed on the support before the material was exposed to the plasma. The activity and selectivity of this material for hydrogenation of acetylene in the presence of ethylene was found to be somewhat better than that observed for catalysts of an identical composition prepared using the standard calcination procedure. There is some improvement noted relative to catalytic material produced in a similar fashion, but calcined using standard thermal approach. Others also report improved catalyst performance after plasma treatment [64,65,66].

Special Fabrications-

In the Complex Nanoparticles section several examples of truly unique nanoparticles production using A-T-P methods were outlined. The A-T-P approach is also a potential alternative for the production of some exciting, but difficult to produce materials (some nano, some larger) such as single wall carbon nanotubes, graphene, spherical ceramics of controlled size, and micron sized metal particles. The technique also has been used to create crystalline spherical boron nitride, clearly a unique material. It is expected that the list of 'special' materials generated using an A-T-P approach will grow, particularly as more scientists become aware of the unique, barely taped, potential of this technology.

Using a variation on the A-T-P method, single wall carbon nanotubes, present as multi-millimeter threads, were generated inside the center of the plasma[67,68]. Carbon nanotubes were grown from a gaseous stream created by passing carbon monoxide over a bed of iron particles. The resulting gas contained CO and iron carbonyl. Apparently, this gas decomposed at the high temperature encountered to form iron particles and C atom fragments from the disproportionation of CO. The difference between the approach

employed and the usual A-T-P process was that the product collected inside the torch, not on downstream filters, and thus could only be harvested after the plasma was off.

A material of even greater interest at present is graphene, a stack of ten or fewer layers of basal planes of graphite. Graphene promises to be an exciting new material of potential value in many applications, making it a material of intense interest[69,70].

Using a simple microwave torch, graphene was generated by passing low concentration of methanol through an atmospheric pressure, low power (250 W) microwave generated argon plasma (Figure 12). The graphene was captured on filter paper downstream, and dissolved in solvent. The authors argued that this is the first technique to create 'free standing' graphene, and in a form that can be re-dispersed [70a]. The other techniques: including micromechanical cleavage of graphite[69,71,72,73,74,75] the chemical reduction of exfoliated graphite oxide [76,77,78] , the vacuum graphitization of silicon carbide substrates[70,79], and the growth of graphene on metal substrates[80,81,82] do not yield readily dispersable graphene.

Often, when applied to small particle ceramics, 'spherical' is an approximation. Yet, spherical shape can be important. For example, the viscosity of a fluid containing true spherical particles is far lower than one containing other shape [83]. This can significantly impact applications such as injection molding of filled polymers. At sufficiently high viscosity, which increases with loading as a function of particle shape, injection molding becomes impractical. In this regard, it appears that A-T-P offers the only route to true spherical shape[84,85] for many high melting temperature ceramics such as alumina (Figure 13). As is passes through the ATP torch, the 'potato' shaped particles melt or soften sufficiently to agglomerate and form spheres.

One of the most popular car colors is silver. This color actually drives from micron sized aluminum particles contained in the paint. At present the standard aluminum

particle size is determined from the mechanics of ball milling. This technology is limited and there is no practical process for ball milling aluminum particles to the size that is most efficient at creating the silver color, about 1 micron. Thus, the current generation of paint contains particles of a non-ideal size, that is particles with an average size greater than 10 micron. Again, the A-T-P process appears to have some unique capability [86]. Controlling the size of particles via techniques that shrink parent feedstock is difficult, but growing particles from a smaller size to a larger size is well understood. Using A-T-P workers showed that aluminum particles of specified size, e.g 1 nm, can be generated by agglomeration of nanoaluminum particles (Figure 14).

One material that apparently can only be generated in a plasma torch[87,88] is crystalline and spherical boron nitride (Figure 15). This material has been sought as a potential ceramic filler for integrated circuit packages because of its high thermal conductivity, but low electrical conductivity. This combination of characteristics is believed to be ideal for thermal management of ICs because it will help carry the heat away without creating an electrical short circuit. BN normally assumes a platelet shape, which is impractical for incorporation into a part fabricated by high solid filled injection molding. Spherical BN is needed. It is noteworthy that a percolation analysis of spherical heat fillers suggests that resistance at point contacts will significantly impede net heat transfer, thus negating the positive characteristics of BN as a filler [89]. The science of spherical BN formation is unusual and suggestive of a possible general use of A-T-P. As with any material, spherical structures of BN form during melting. Generally, BN does not melt, but rather sublimates at sufficient temperature. However, in a plasma containing a significant pressure of N atoms, the decomposition temperature is increased (Fig. 16). Thus, the melting temperature (not precisely known) can be reached before the BN decomposes.

This leads to the formation of spherical particles in a high temperature, high N atom, plasma, such as can be produced with a microwave system from N_2 gas.

Some truly remarkable phase and unique separations have been observed. For example ceria-alumina particles in which the surface is clearly divided into ceria rich and alumina rich areas [58] were produced (Fig 17). There may be some eventually chemical applications, possibly in catalysis, for particles with such unique and localized segregation. One final aspect of A-T-P treated materials is the apparent ability of the technique to purify materials. There is clear evidence that ceramics that are treated with the A-T-P method are of a higher purity than the input materials[90].

CHARACTERIZATION AND MODELING

Full advantage of the A-T-P process requires a reasonably sophisticated understanding of the nature of the plasmas employed. Indeed, the plasmas employed are not merely 'high temperature flames', but rather remarkably complex structures in which even the term 'temperature' cannot be used with impunity. Moreover, from the perspective of material science it is exciting that extremely high 'temperature' can be achieved in both oxidizing and reducing environments, the population of radicals can be 'controlled' (e.g. high concentrations of N, C, O and H atoms), and environments change rapidly with position allowing for a choice of 'injection' points. Exploitation of these and other aspects of atmospheric pressure plasma torches have hardly been fully explored for novel material synthesis.

There are few characterization studies, but they show some remarkably interesting phenomenon. For example, it has been shown that the afterglow of atmospheric pressure

plasmas containing particles have vastly different characteristics than identical plasmas containing no aerosol particles [91]. In particular, both the charged and neutral temperature are more than twice as high in the presence of low concentrations of alumina particles (<1% by volume) than they are in the absence of particles with aerosol (Fig. 18). Even the shape of the temperature profiles are different (Fig 19). Several groups have shown that in the absence of aerosol particles, the highest temperature in the afterglow is 'isolated' above the power source[92,93,94]. In the presence of particles the isotherms appear to look as intuitively anticipated: highest at the center and decaying with distance from the power source. Many questions are raised by this result: Is this only true in microwave systems? Is this a function of the nature of the particles? Do the particles fundamentally change the flow pattern?

One fundamental experimental result that has been observed repeatedly is that the local thermodynamic equilibrium model (LTE) does not apply even to the afterglows of atmospheric pressure systems. It is quite clear both in A-T-P and in high pressure 'bell jar' plasmas [95,96] that charged species temperatures are many times higher than the neutral species temperatures.

In early models/simulations of A-T-P plasmas[3437,38,97,98], a single temperature was sufficient to describe all species, as per the textbook, LTE-like approach[3]. This approach cannot produce models consistent with data, at least for microwave generated plasmas, hence novel models were developed. To model the afterglow of a microwave generated plasma a 'two system' approach was devised[99,100,101,102]. Separate transport equations

were solved for two 'sub-systems': 'neutral' and 'charged'. This implies that two systems occupy the same space at the same time. Mathematically, the two transport equations 'couple' only in the 'generation' terms. For example, the charged species equations require a local input of the neutral species concentrations, and temperature, in order to determine the rate of generation of new charged species, and concomitantly new neutral species (e.g. radicals). This new approach yielded remarkable insight. For example, it was found that charged species transport is dominated by diffusion and in the same plasma neutral transport is dominated by convection. The agreement with data was excellent in all cases tested.

A new modeling approach was also applied to the high field ('coupler') zone of microwave generated plasmas[103]. For example, in one case a zero dimensional model was employed that required a multi-step approach. In the first step the Boltzmann equation is solved for the electron energy distribution function (EEDF). This is next used to calculate rate constants for electron-neutral collisions. These values are then used to solve a zero dimensional system of chemical reactions. Once this set is solved, the results can be put in an energy balance, the output of which is the neutral (gas) species temperature. A power balance is then employed to test for self-consistency. If the system is not self consistent, the input parameters to the EEDF are modified, and the computational process repeated. More recently, variations on this approach have been employed for other plasma systems[95,96].

SUMMARY

The first efforts at creating unique materials using A-T-P methods, generally using high power RF plasmas, were recorded more than thirty years ago. Although those efforts were successful, mostly in producing nano-ceramic particles from gaseous precursors, they were not sustained. Over the last decade more persistent efforts, often using low power microwave plasma sources, and a wide range of precursor materials, have demonstrated the diversity of nano-scale and particulate materials that can be generated using the A-T-P approach. Among the more interesting, and arguably unique, materials generated are multi-layer (complex) nanoparticles, sinter resistant ceramics, spherical crystalline BN, carbon-graphite coated metal particles, single wall carbon nanotubes in vast quantity, free standing graphene, and supported metal catalysts with unique catalytic properties. The 'scalability' to commercial viability has yet to be demonstrated, although development efforts in industry are nearing maturity.

A surprising outcome of the work is the discovery of the vast influence of particles, even in very low volume, on every characteristic of the afterglow portion of the plasma including electron temperature, electron density, temperature profiles and even neutral temperatures. These findings have led to the development of some novel modeling approaches, including presuming the plasma is composed of weakly coupled sub-systems, one charged, and one neutral. Two transport equations must be solved, and each produces a separate temperature profile in agreement with data.

REFERENCES

1. R. J. Shul and S. J. Pearton, 'Handbook of Advanced Plasma Processing Techniques', Springer 2000.
2. B. Chapman, 'Glow Discharge Processes: Sputtering and Plasma Etching', Wiley-Interscience (1980).

3. M. A. Lieberman and A.J. Lichtenberg, 'Principles of Plasma Discharges and Materials Processing, 2nd Edi', Wiley-Interscience (2005).
4. J. Mort, F. Jansen, 'Plasma Deposited Thin Films', CRC Press (2000).
5. R. B. Heimann, 'Plasma Spray Coating: Principles and Applications', Wiley –VCH (2008).
6. S. H. Anastasiadis, A. Karim and S. S. Ferguson, eds.'Interfaces, Adhesion and Processing in Polymer Systems' (MRS Vol. 629), Materials Research Society, 2001.
7. R. d'Agostino, P. Favia, and Y. Kawai, 'Advanced Plasma Technology', Wiley-VCH Verlag GmbH (2008).
8. C, Tendero, C. Tixier, P. Tristant, J. Desmaison, P. Leprince, *Spectrochimica Acta* B 61, **2006**.
9. W.J.M. Mulder, G.J. Strijkers, G. A.F. vanTilborg, A. W. Griffioen, K. Nicolay, *NMR in Biomedicine* **19**, 142 (2006).
10. M.E. McHenry, S. A. Majetich and E. M. Brunsman, *Mat. Sci. And Engr.***A 204**, 19 (1995).
11. J. W.M. Bulte,and M. M.J. Modo, 'Nanoparticles in Biomediacal Imaging: Emerging Technologies and Applications', Springer, NY (2008).
12. K. Kimoto; Y. Kamiya; M. Nonoyama; R. Uyeda, *Jpn. J. Appl.Phys.* **1963**, *2*, 702-713.
13. W. Gong; H. Li.; Z.G. Zhao; Chen, J. C. *J. Appl. Phys.* **1991**, *69*, 5119-5121.
14. S. Iwama; K. Hayakawa, *Nanostruct. Mater.* **1992**, *1*, 113-118.
15. S. Panda; S.E. Pratsinis, *Nanostruct. Mater.* **1995**, *5*, 755-767.
16. H.J. Fecht, *Nanostruct. Mater.* **1992**, *1*, 125-130.
17. V. Haas; R. Birringer, *Nanostruct. Mater.* **1992**, *1*, 491-504.
18. J.A. Eastman; L.J. Thompson; D.J. Marshall, *Nanostruct. Mater.*, **1993**, *2*, 377-382.
19. P.J. Herley; W. Jones, *Nanostruct. Mater.* **1993**, *2*, 553-562.
20. K. Recknagle; Q. Xia; J.N. Chung; C.T. Crowe; H. Hamilton; G.S. Collins, *Nanostruct. Mater.* **1994**, *4*, 103-111.
21. J.P. Chen; C.M. Sorensen; K.J. Klabunde; G.C. Hadjipanayis; E. Devlin; A. Kostikas, *Phys. Re*V. *B* **1995**, *51*, 11527-11532.
22. T. Yamamoto; J. Mazumder, *Nanostruct. Mater.* **1996**, *7*, 305-312.
23. T. Majima; T. Miyahara; K. Haneda; T. Ishii; M. Takami, *Jpn, J. Appl. Phys.* **1994**, *33*, 4759-4763.
24. Y. Sawada; Y. Kageyama; M. Iwata; A. Tasaki, *Jpn. J. Appl.Phys.* **1992**, *31*, 3858-3861.
25. R. Mueller, R. Jossen, S. E. Pratsinis, M. Watson and M. K. Akhtar, *J. Am. Ceram. Soc.*, **2004**, 87, 197.
26. R. Strobel, S.E. Pratsinis, *J. Mater. Chem.*, **2007**, 17, 4743–4756
27. R. N. Grass, and W. Stark, *J. Mater. Chem.*, **2006**, 16, 1825–1830
28. G. L. Messing, S.C. Zhang, and G.V. Jayanthi, *J. Am. Cer. Soc.* 76, 2707, **1993**.
29. A. Gurav, T. Kodas, T. Pluym, Y. Xiong, *Aerosol Sci. and Tech.* 19, 411, **1993**.
30. W.J. Stark and S. E. Pratsinis, *Powder Techn.* 126, 103, **2002**.
31. I. M. MacKinnon and B. G. Reuben, *J. Electrochem Soc.*, 122, 806, **1975**.
32. I. M. Mac Kinnon and A. J. Wickens, *Chemistry in Industry* 800, 1, **1973**.
33. C. M. Hallabaugh, D. E. Hull, L.R. Newkirk and J. J. Petrovic, *J. Mat. Sci.* **18**, 3190 (1983).

34. T. Yoshida, A. Kawasaki, K. Nakagawa, and K. Akashi, *J. Mater. Sci.* 14, 1624 (1979).
35. C.H Chou and J. Phillips. *J. Mat. Res.* 7, 2107, **1992**.
36. J. R. Brenner, J.B. L. Harkness, M. B. Knickelbein, G. K. Krumdick and C.L. Marshall, *Nanostructured Materials* **8**, 1, (1997).
37. S.L. Girshick, C-P Chin, R Muno, C. Y. Wu, L. Yang, S.K. Singh and P.H. McMurry, *J. Aero. Sci.* 24, 367, **1993**.
38. N. Rao, S. Girshick, J. Heberlein, P. McMurry, S. Jones,D. Hansen and B. Micheel, *Plasma Chem and Plasma Proc.* 15, 581, **1995**
39. S.L. Girshick and C.-P. Chiu, *Plasma Chem. and Plasma Proc.* 9, 355, **1989**.
40. J. C. Weigle, C.C. Luhrs, C. K. Chen, W.L. Perry, J.T. Mang, M.B. Nemer, G.P. Lopez, J. Phillips, *J. Phys. Chem. B* **2004**, *108,* 18601-18607.
41. M. Frenklach; H. Wang, In *Soot Formation in Combustion:Mechanisms and Models*; Bockhorn, H., Ed.; Springer-Verlag: Berlin, **1994**; 162-190.
42. N.L. Wu; J. Phillips, *J. Catal.* **1988**, *113*, 129-143.
43. B. Zhao; Z. Yang; M.V. Johnson; H. Wang; A.S. Wexler; M. Balthasar; M. Kraft, *Combust. Flame* **133**, 173 (2003).
44. G. Vanamu; K. Lester; A.K. Datye; J.C. Weigle; C.K. Chen; D. Kelly; J. Phillips, *AIChE J.* **2004**, *50*, 2090.
45. T. Matsoukas; M. Russell, *J. Appl. Phys.* **1995**, *77*, 4285-4292.
46. J. Phillips, D. Mendoza, C.K. Chen, (2008). 'Method for Producing Metal Oxide Nanoparticles', *U.S Patent* 7,357,910.
47. R. Bardhan, N. K. Grady, N. J. Halas, *Small,* 4(10) 1716-1722 **2008**.
48. M.-R. Choi, K.J. Stanton-Maxey, J.K. Stanley, C.S. Levin, R. Bardhan, D. Akin, S. Badve, J. Sturgis, J. P. Robinson, R. Bashir, N.J. Halas, S.E. Clare, *Nano Letters* 7(12) 3759-3765, **2007**.
49. Z. Wen, Q. Wang, Q. Zhang, J. Li, *Electrochemistry Communications*, **2007**, 9, 1867–1872.
50. J. Phillips, T. Shiina, M. Nemer, K. Lester, *Langmuir* **22**, 9694 (2006).
51. G.L. Hwang, 'Preparation of Hollow Carbon Nanocapsules' US Patent 7,156,958 (2007).
52. J. Phillips, L. Cheng, C. Luhrs, H. Zea, M. Courtney, C. Hanson, Mater. Res. Soc. Symp. Proc. Volume 1056E, Warrendale, PA,, #HH08-42, 2008.
53. J. Phillips, C. Luhrs and P. Fanson, *Langmuir* **23**, 1315, 2007.
54. A. Trovarelli, *Catal. Rev. Sci. Eng.* **38** , 439 1996.
55. M. Shelef; R.W. McCabe, *Catal. Today* **62**, *35* 2000..
56. H. Schulz; W.J. Stark; M. Maciejewski; S.E. Pratsinis; A. Baiker, *J. Mater. Chem.* **2003**, 2979-2984
57. Kubaschewski and Hopkins, '*Oxidation of Metals and Alloys*', Butterworths, London 1962.
58. J. Phillips, C. Luhrs, C. Peng, and P. Fanson, 'Engineering Aerosol-Through-Plasma Torch Ceramic Particulate Structures: Influence of Precursor Composition', *J. Mat Res.* **23**, 1870 (2008).
59. C. C. Luhrs, J. Phillips and P. Fanson, 'Production of Unique Structures Using the Aerosol Through Plasma Process', *WIT trans. On the Built Env.* **97**, 63 (2008).
60. J. Phillips, 'Plasma Generation of Supported Metal Catalysts', U.S. Patent *5,989,648*
61. J. Phillips, S. Shim, I. M. Fonseca, S. Carabineiro, *Applied Catalysis* **237**, 41-51,

2002.
62. H. Zea, C.-K. Chen, K. Lester, A. Phillips, A. Datye, I. Fonseca. J. Phillips, *Catalysis Today* **89**, 237, 2004.
63. C. Shi, B.W-L. Jang, *Ind. Eng. Chem. Res.*, **2006**, 45, 5879-5884.
64. C. Ratanatawanate, M. Macias, B.W.-L. Jang, *Ind. Eng. Chem. Res.*, **2005**, 44, 9868
65. C. Liu, J. Zou, K. Yu, D. Cheng, Y. Han, J. Zhan, C. Ratanatawanate, B. W.-L. Jang, *Pure Appl, Chem* (in press)
66. J.-J. Zou, C.-J. Liu, Y.-P Zhang, *Langmuir*, **2006**, 22, 2334.
67. J. Phillips, W.L Perry, C.K. Chen, 'Plasma Method for Producing Carbon Nanotubes', *U. S. Patent 6,998,103* (**2006**).
68. C.-K. Chen, W.L. Perry, J. Phillips, *Carbon* 41, 2555, **2003**.
69. K.S. Novoselov, A.K. Geim, S.V. Morozov, D. Jiang, Y. Zhang S.V. Dubonos, I.V. Grigorieva, A.A. Firsov, *Science* **2004**, *306*, 666.
70. J. Hass, R. Feng, T. Li, X. Li, Z. Zong, W.A. de Heer, P.N. First, E.H. Conrad, C.A. Jeffrey, C. Berger, *Appl. Phys. Lett.* **2006**, *89*, 143106.

70a. Albert Dato, Velimir Radmilovic, Zonghoon Lee, Jonathan Phillips and Michael Frenklach, 'Substrate-Free Gas-Phase Synthesis of Graphene Sheets' *Nano-Letters* **8**, 2012 (2008).

71. K.S. Novoselov, D. Jiang, F. Schiedin, T.J. Booth, V.V. Khotevich, S.V. Morozov, A.K. Geim, *Proc. Natl. Acad. Sci. U.S.A.* **2005**, *102*, 10451.
72. K.S. Novoselov, A.K. Geim, S.V. Morozov, D. Jiang, M.I. Katsnelson, I.V. Grigorieva, S.V. Dubonos, A.A. Firsov, *Nature* **2005**, *438*, 197.
73. K.S. Novoselov, E. McCann, S.V. Morozov, V.I. Fal'ko, M.I. Katsnelson, U. Zeitler, D. Jiang, F. Schedin, A.K. Geim, *Nat. Phys.* **2006**, *2*, 177.
74. J.C. Meyer, A.K. Geim, M.I. Katsnelson, K.S. Novoselov, T.J. Booth, S. Roth, *Nature* **2007**, *446*, 60.
75. A.C. Ferrari, J.C. Meyer, V. Scardaci, C. Casiraghi, M. Lazzeri, F. Mauri, S. Piscanec, D. Jiang, K.S. Novoselov, S. Roth, A.K. Geim, *Phys. Re*V. *Lett.* **2006**, *97*, 187401.
76. S. Stankovich, D.A. Dikin, G.H.B. Dommett, K.M. Kohlhaas, E.J. Zimney, E.A. Stach, R.D. Piner, S.T. Nguyen, R.S. Ruoff, *Nature* **2006**, *442*, 282.
77. S. Stankovich, D.A. Dikin, R.D. Piner, K.A. Kohlhaas, A. Kleinhammes, J. Yuanyuan, Y. Wu, S.T. Nguyen, R.S. Ruoff, *Carbon* **2007**, *45*, 1558.
78. K.N Kudin, B. Ozbas, H.C. Schniepp, R.K. Prud'homme, I.A. Aksay, R. Car, *Nano Lett.* **2008**, *8*, 36.
79. C. Berger, Z. Song, X. Li, X. Wu, N. Brown, C. Naud, D. Mayou, T. Li, J. Hass, A.N. Marchenkov, A.H. Conrad, P.N. First, W.A. de Heer, *Science* **2006**, *312*, 1191.
80. J. Coraux, A.T. N'Diaye, C. Busse, T. Michely, *Nano Lett.* **2008**, *8*, 565.
81. S. Marchini, S. Gu¨nther, J. Wintterlin, J. *Phys. Re*V. *B* **2007**, *76*, 075429.
82. H. Ueta, M. Saida, C. Nakai, Y. Yamada, M. Sasaki, S. Yamamoto, *Surf. Sci.* **2004**, *560*, 183.
83. L.V. Berlyand, D. Golovaty, A. B. Movchan, J. Phillips, *Quarterly Journal of Mechanics and Applied Mathematics* 57, 495-528 **2004**.
84. J. Phillips, S. Gleiman, C.-K. Chen. 2001. 'Method for Producing Ceramic Particles and Agglomerates,' *U.S. Patent 6,261,484 B1*.
85. J.Phillips, S. Gleiman, C.K. Chen, *J. of Mat. Res.* 16,1256, **2001**

86. J. Phillips, W. Kroenke, W.L. Perry. (2004). 'Method for Producing Metallic Microparticles', *U.S. Patent* 6,755,886.
87. J. Phillips, S. Gleiman, C.K. Chen. 2003. 'Method For Preparing Spherical Particles Of Boron Nitride', *U. S. Patent 6,652,822.*
88. S. Gleiman, C.-K. Chen, A. Datye, J. Phillips, *Journal of Materials Science*, 37 (16), 3429-3440, **2002**
89. D. Gerenrot, L. Berlyand, J.Phillips, *IEEE Transactions on Advanced Packaging,* 26, 1521, **2003**
90. G. Vanamu, K. Lester, A. Datye, J. Weigle, C.-K. Chen, J.Phillips, *AIChE J*, 50, 2090, **2004**
91. C.-K. Chen, J. Phillips, 2002, *J. Phys. D: Applied Physics*, 35. 998-1009, **2002**
92. M. Huang, D.S. Hanselman, Q. Jin, G.M. Hieftje, *Spectrochim. Acta*, B45, 1339, **1990**
93. N.H. Bings, M. Olschewski, J.A.C. Broekaert, *Spectrochim. Acta* B52, 1965, **1997**
94. C. Prokisch, A.M. Bilgic, E. Voges, J.A.C. Broekaert, J. Jonkers, M. van Sande, J.A.M. van der Mullen, *Spectrochim. Acta*, B54, 1253, **1999**.
95. T. Farouk, B. Farouk, D. Staack, A. Gutsol, A. Fridman, *Plasma Sources Sci. Technol.* 16, **2007**, 619–634.
96. K Hassouni, A Gicquel, M Capitelli, J. Loureiro, *Plasma Sources Sci. Technol.* 8, **1999,** 494–512. Printed in the UK
97. S.L. Girshick, C.-P. Chiu, P. H. McMurry, *Plasma Chem Plasma Proc.* 8, 145, **1988**.
98. T. Yoshida, T. Tani, H. Nishimura and K. Akashi, *J. Appl. Phys.* **54**, 640 (1983).
99. T.-C. Wei, L. R. Collins, J. Phillips. *J. Phys. D.: Appl. Phys.* **28**:295-304, **1995**
100. T.-C. Wei, L. R. Collins, J. Phillips, *AIChE J.,* 42(5):1361-1370, **1996**
101. J. Phillips, C. H. Chou, T. C. Wei, *Materials Modification by Energetic Atoms and Ions*, Materials Research Society Symp. Proc., 268, 49-55, **1992**
102. C.H. Chou, T.-C. Wei, J. Phillips, *J. Appl. Phy.* 72:870-878, **1992**
103. C.-K. Chen, T-C Wei, L.R. Collins, J. Phillips, *J. Phys. D: Appl. Phys.,* **32**(6):688-698. 1999

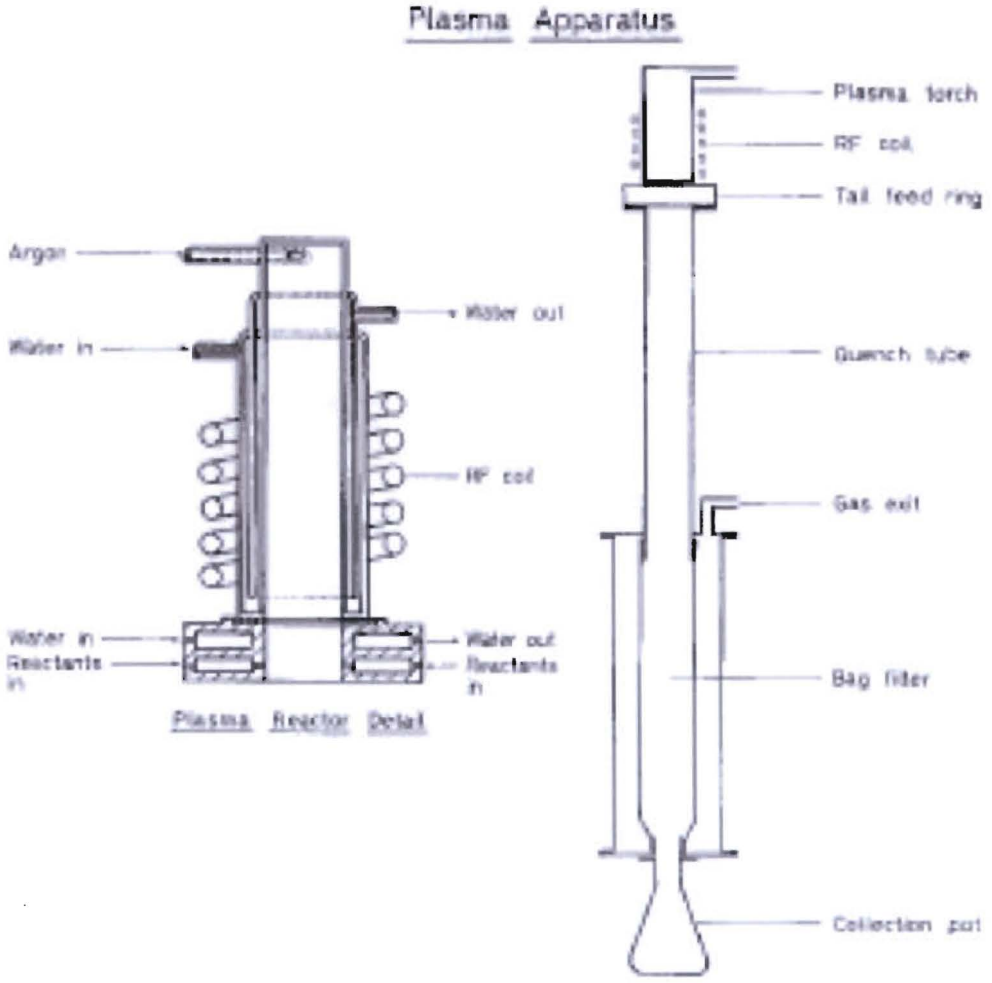

Figure 1: *Typical High Power RF System.* Ceramic particles were generated from gases passed though the RF coupler region, and captured downstream with a filter31

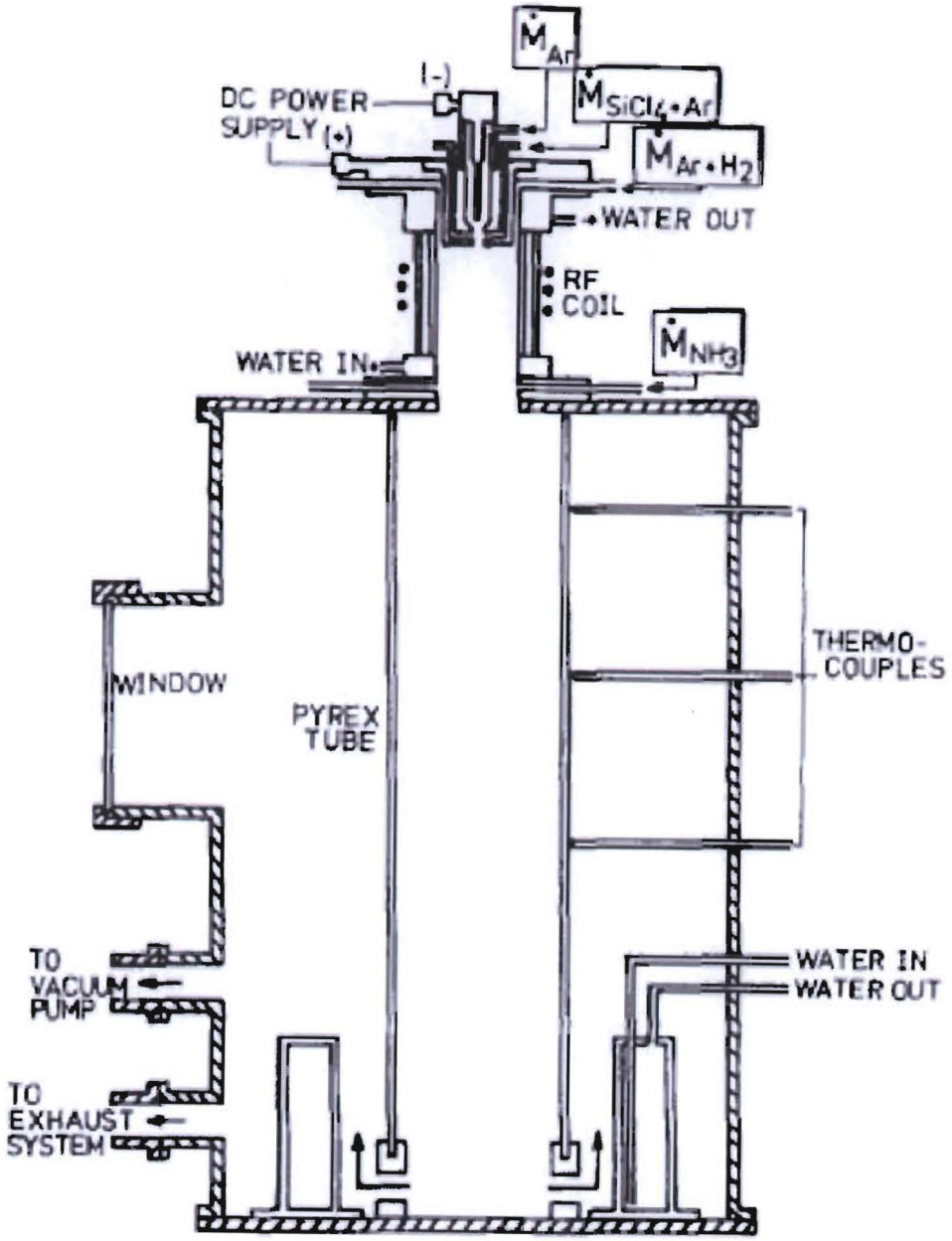

FIG. 8. Schematic view of a reactor chamber designed for the preparation of ultrafine Si_3N_4.

Figure 2- *Hybrid Plasma Torch.* Precursors passed first through a DC discharge, and then an RF system. Early A-T-P systems were always high power RF (>10 kW) and frequently complex34

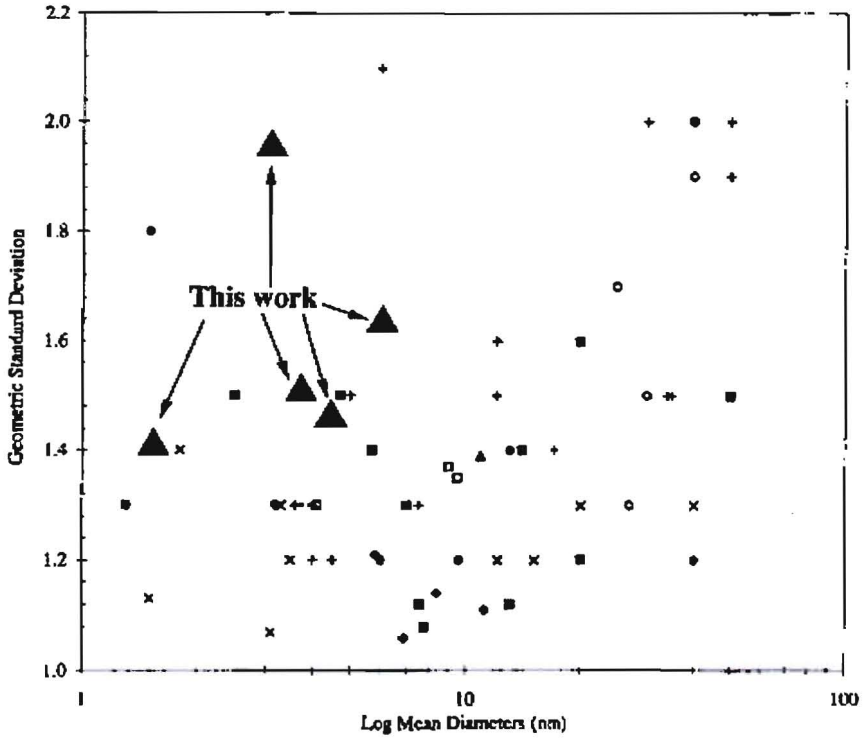

Figure 12. Comparison of the log mean particle diameters and particle size distribution breadths (expressed as the geometric standard deviation) for our microwave plasma-generated particles (▲) with those produced via the following methods: (♦) thermal dissociation of metal carbonyls (24-25, 49-50), (■) laser pyrolysis of metal carbonyls (13-16, 26-30, 48), (+) gas evaporation of metals (21, 31-37) and metal carbonyls (20,22), (x) inverse micelles (17-19, 38-40, 51), (o) other plasma-based methods (31, 41, 47), (❑) impregnation onto high surface area oxides (1-3), (◊) ion exchange into microporous materials (4), and (●) methods not amenable to the generation of nanoparticles that could be used as catalysts (42-46).

Figure 3- *Production of Nanoparticles.* Nanoparticles geanerated from molecular precursors passed through a low pressure microwave plasma compared well, in terms of size with those produced using a host of other methods36.

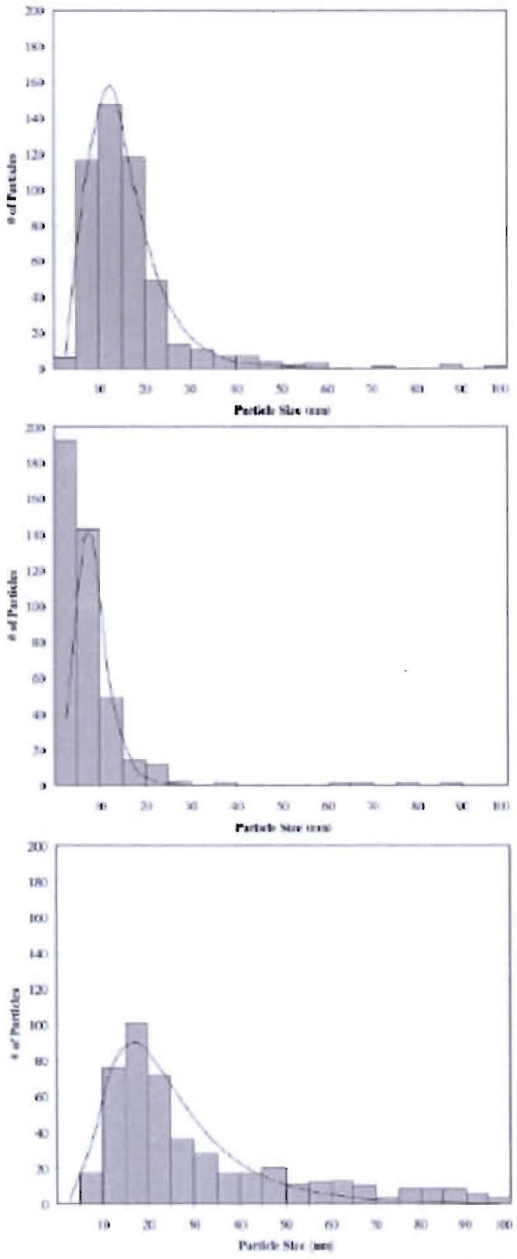

Figure 4. Various types of particle size distributions formed in the plasma torch. (a, top) log-normal distribution, sample G; (b, middle) non-log normal distribution showing more small particles than expected, sample I, (c, bottom) non-log-normal distribution showing more large particles than expected, sample C.

Figure 4: *Particle Size Distributions*. Particle size distributions of nano-metal particles are often not well described by any theory of particle growth40

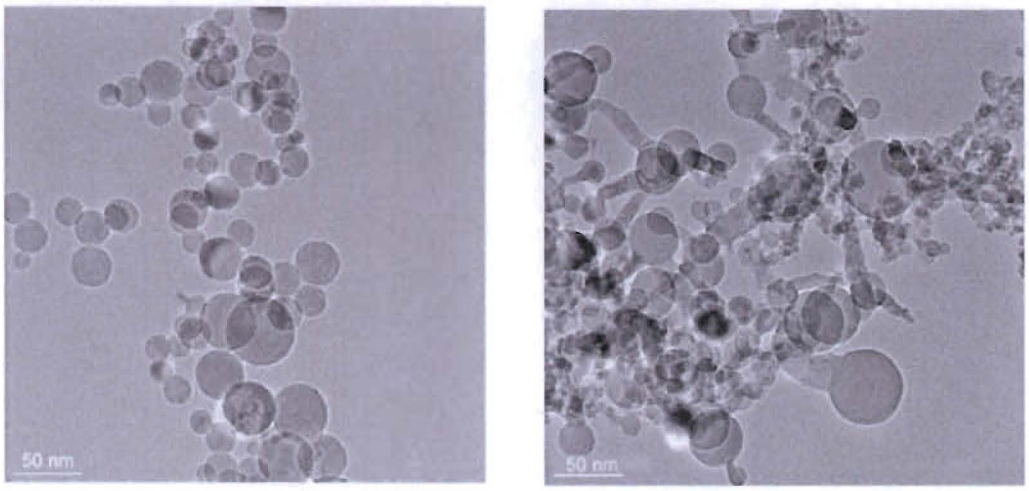

Figure 5- *Aluminum Nanoparticles Formed with A-T-P.* On the left are spherical aluminum nanoparticles, and on the right aluminum nanoparticles with tails40

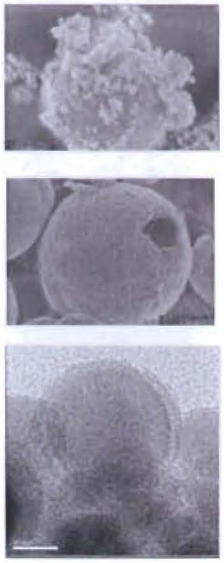

Figure 6: *Ce-Al Ceramic Oxide Particles Produced with A-T-P*. TOP: A bimodal distribution of particles formed. MIDDLE: The larger particles (ca. 10 micron diameter) were mostly hollow. BOTTOM: The nanoparticles (ca. 10 nm diameter) had a shell of alumina and a core of ceria [53].

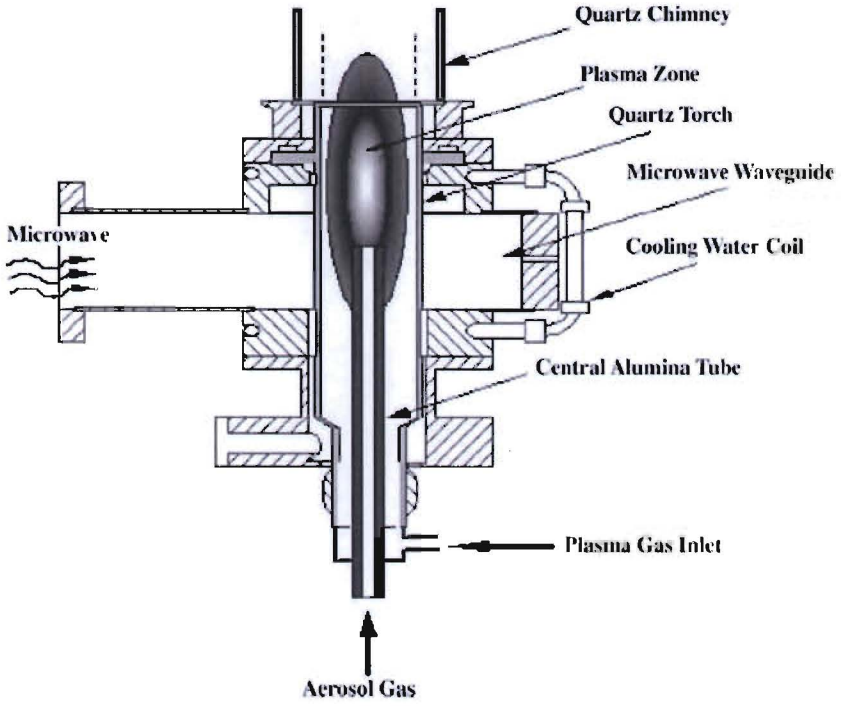

FIG. 1. Schematic representation of coupler region of the microwave plasma torch

J. Mater. Res., Vol. 23, No. 7, Jul 2008

Figure 7- *Microwave Torch Schematic*. Note that the particles are injected as an aerosol with one gas stream to the center of the waveguide through an alumina tube, and a second gas stream (Plasma Gas) is injected from below and around the outside of the alumina tube. The quartz reactor is about 18 mm OD [58].

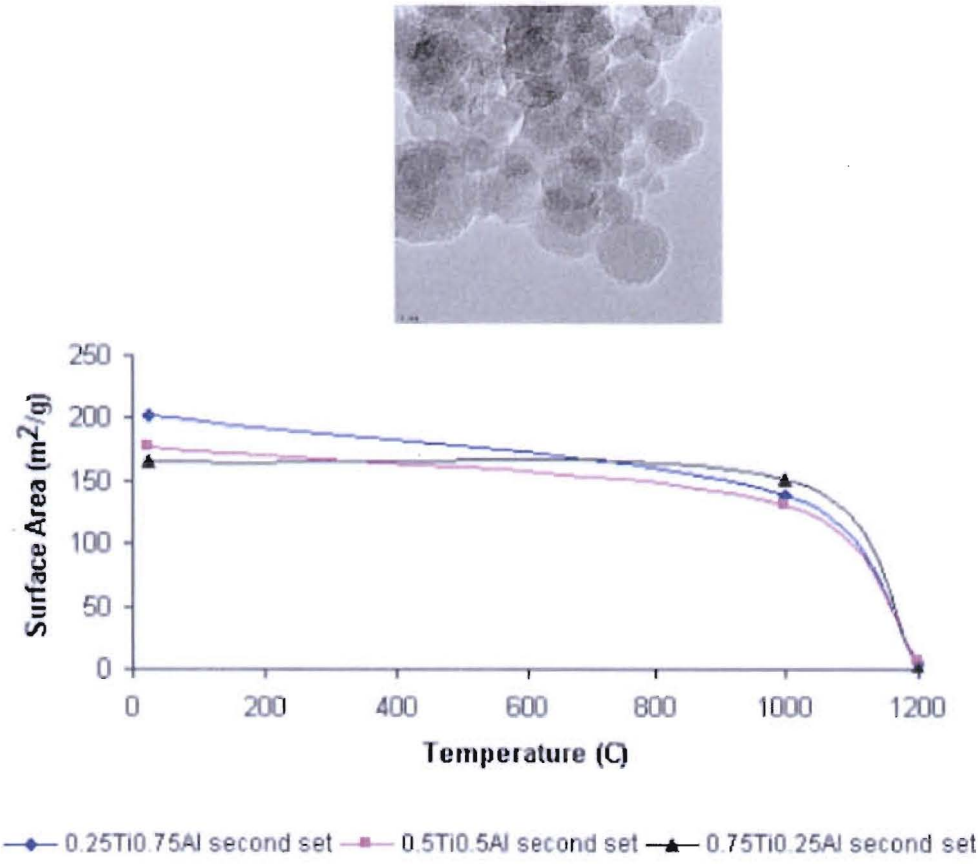

Figure 8- *Titania/alumina Particles*. These highly crystallized particles (inset) proved to have remarkable thermal stability, loosing little surface area even after sintering at 1000 C in oxygen for five hours52

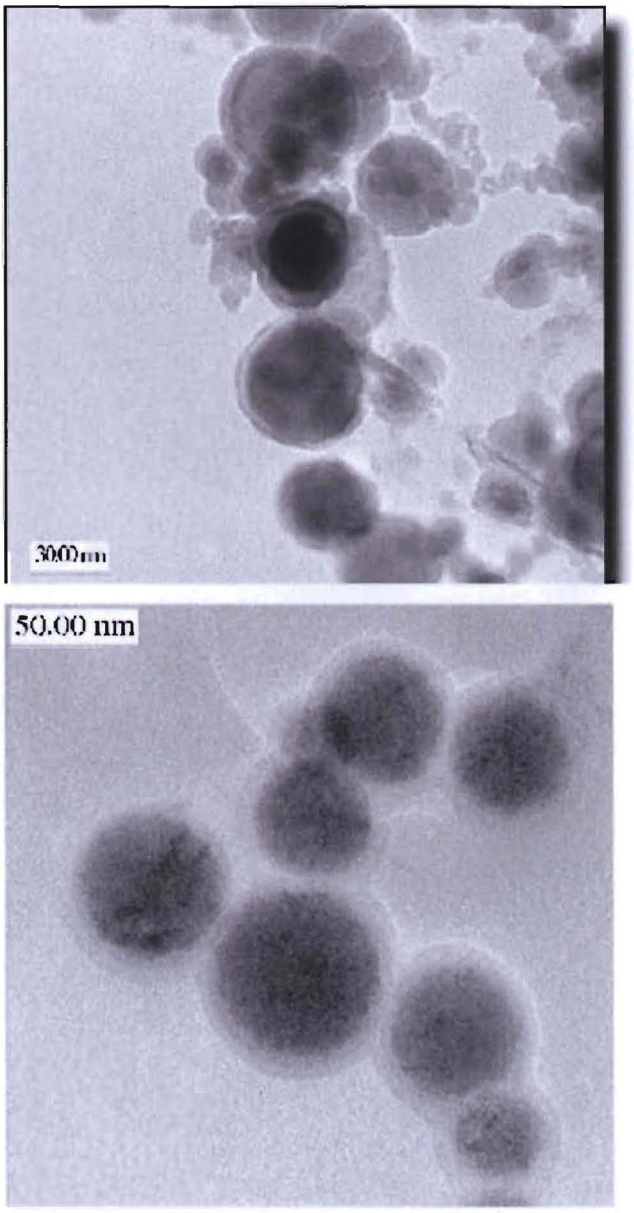

Figure 9-*Carbon-Graphite Coated Metal.* The A-T-P process for creating core metal/shell carbon-graphite works for a variety of metals and carbon precursors. TOP- Sn core particles generated from micron tin particles and hexane vapor. BOTTOM- Al core particles generated from micron aluminum particles and anthracene powder. Using methanol or ethylene as the carbon source produced similar, albeit with less graphitized shells, particles.

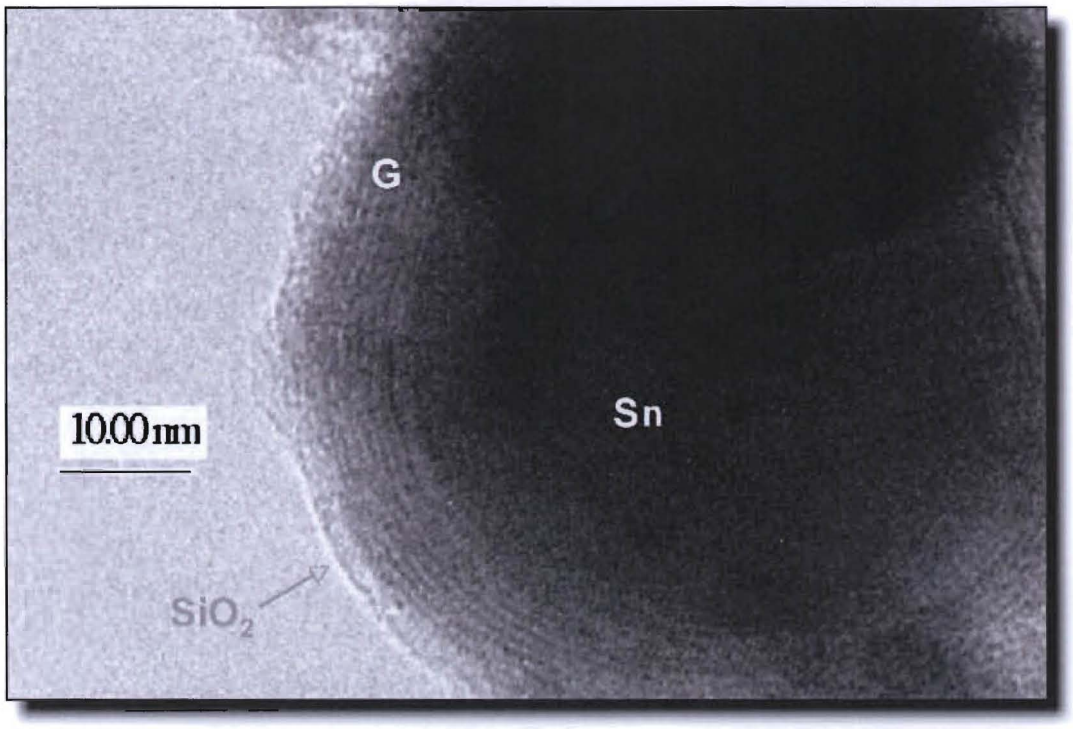

Figure 10- *Tri-Layer Particle*. Metallic tin (Sn) core/carbon-graphite (G) nano particles were generated with the A-T-P method, and a third layer (SiO2) deposited in a post-plasma treatment.

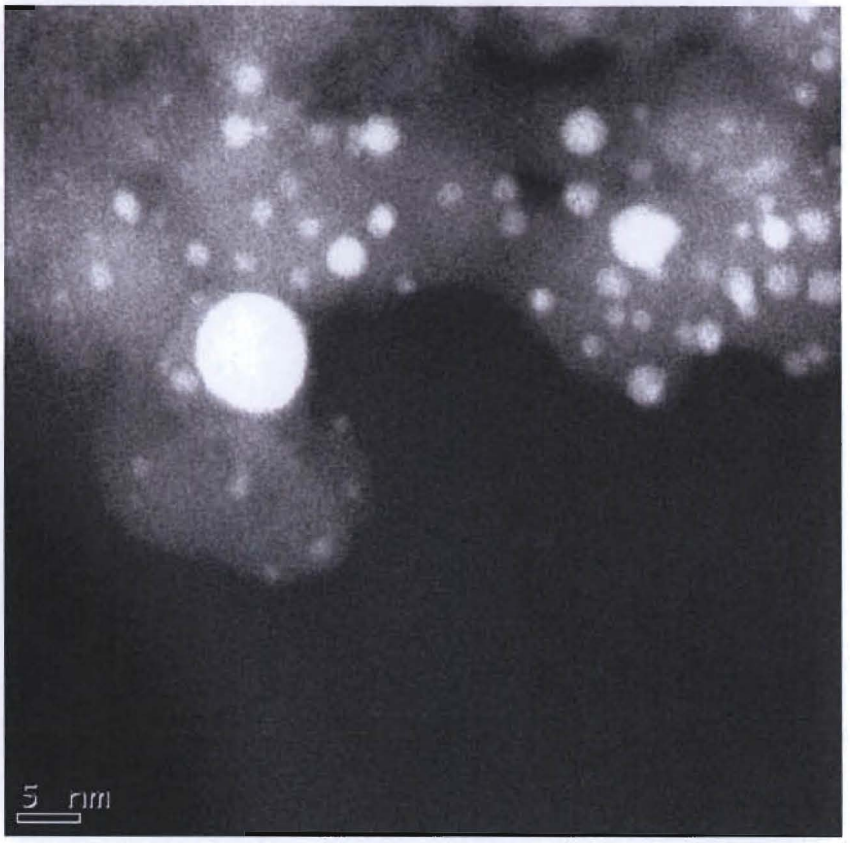

Figure 11- *Pd/C Catalysts by TEM.* Pd/C catalysts produced with 600 W of power using the A-T-P method had an average particle size, from micrographs, of 2.5 nm, and a dispersion (selective chemisorption) of ~60%. This is exceptionally high dispersion for carbon supported catalysts [62].

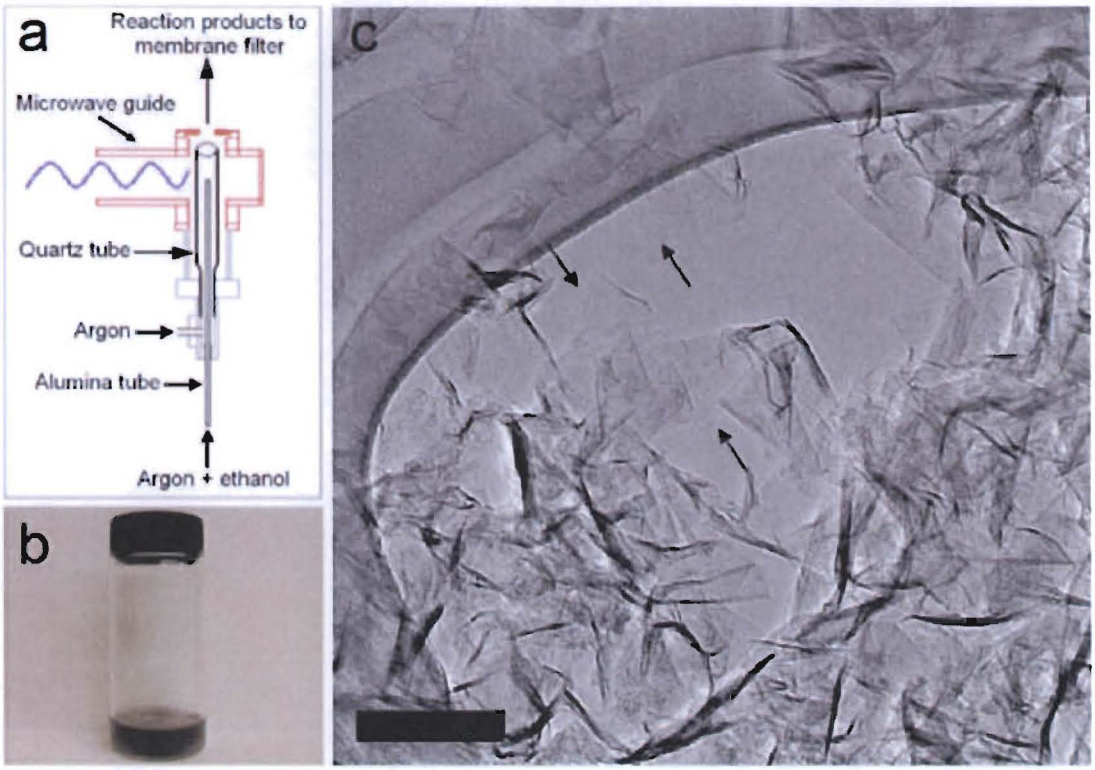

Figure 12. *Synthesis of graphene sheets.* (a) Schematic of the atmospheric-pressure microwave plasma reactor used to synthesize grapheme; (b) Photograph of graphene sheets dispersed in methanol. (c) A typical TEM image of graphene sheets freely suspended on a lacey carbon TEM grid. Homogeneous and featureless regions (indicated by arrows) indicate regions of monolayer graphene. Scale bar represents100 nm [70a].

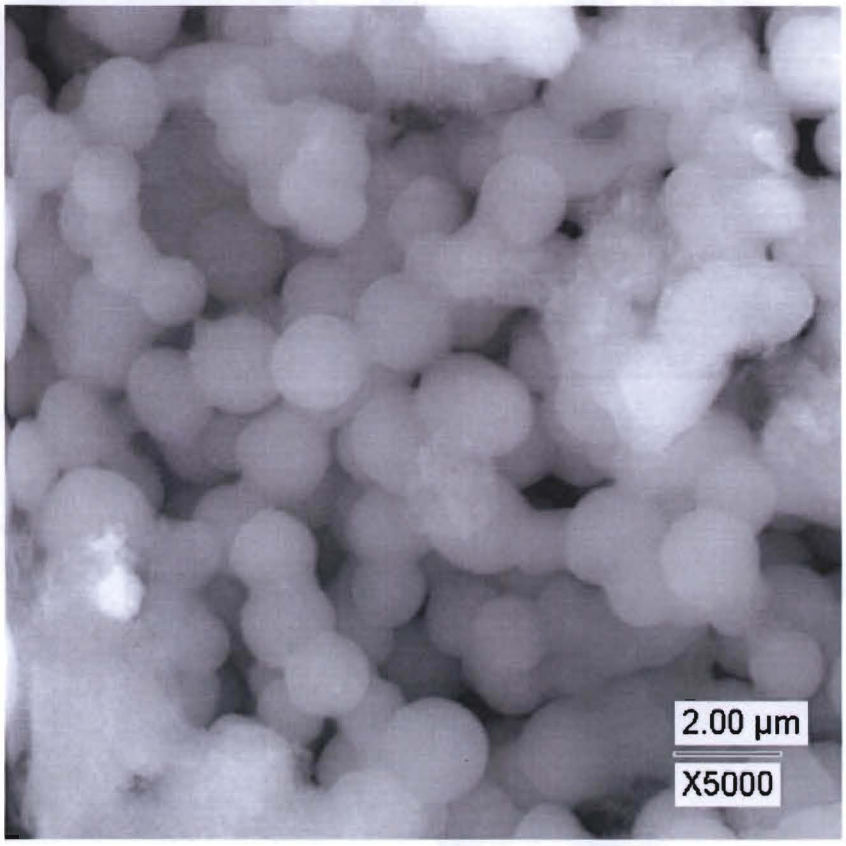

Figure 13 *Micron Aluminum*. Micron sized aluminum particles were generated from nanoaluminum particles86

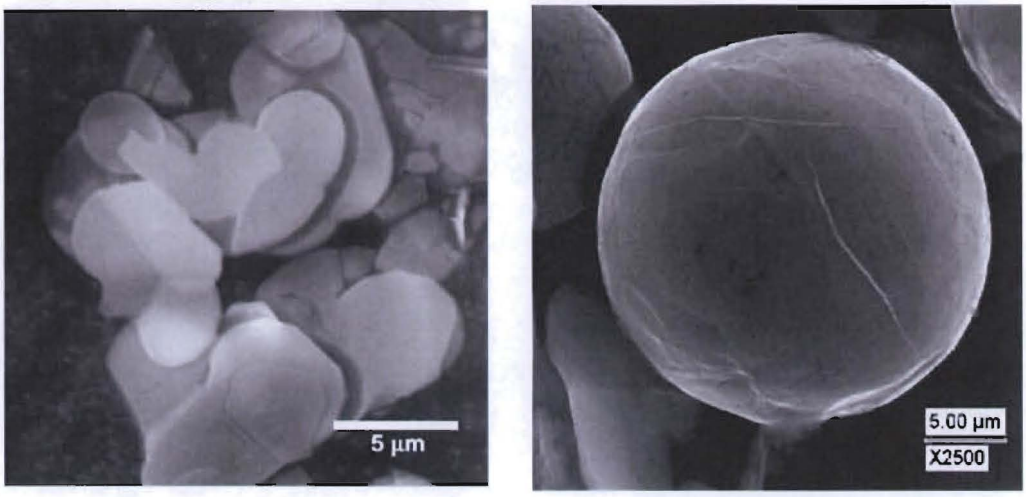

Figure 14- BN Spherodization: LEFT: In an argon only plasma BN morphology is unchanged from the platelet structure of the precursor. RIGHT: In a pure N_2 plasma spherical BN forms [88].

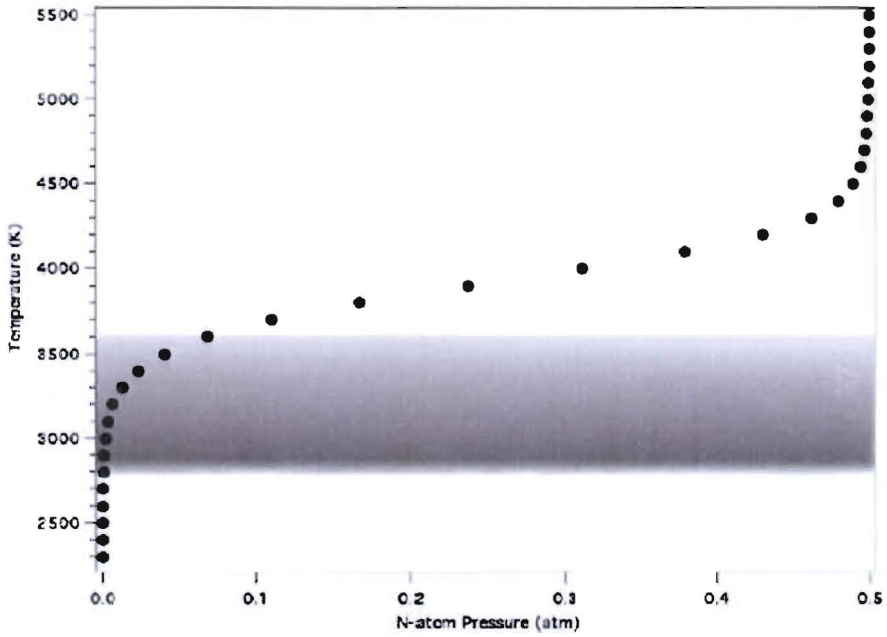

Figure 7 Boron nitride decomposition temperature as a function of N-atom pressure. Because the melting temperature of hBN is not well known, the shaded area from approximately 2800 K is used to denote a possible melting region. Beyond an N-atom pressure of approximately 0.1 atm, the decomposition temperature is elevated significantly beyond the melting temperature. N-atom pressures of 0.25 atm and higher are possible while processing in an atmospheric pressure nitrogen plasma.

Figure 16- BN Decomposition Temperature as a Function of N atom Pressure. At sufficiently high N atom pressure BN will melt rather than decompose[88].

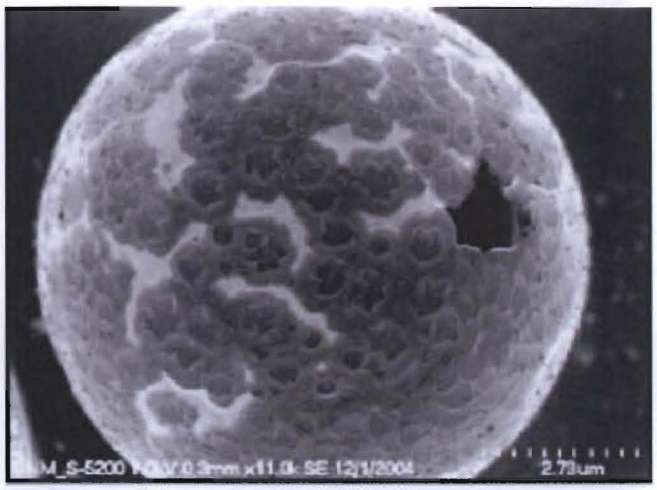

(a)

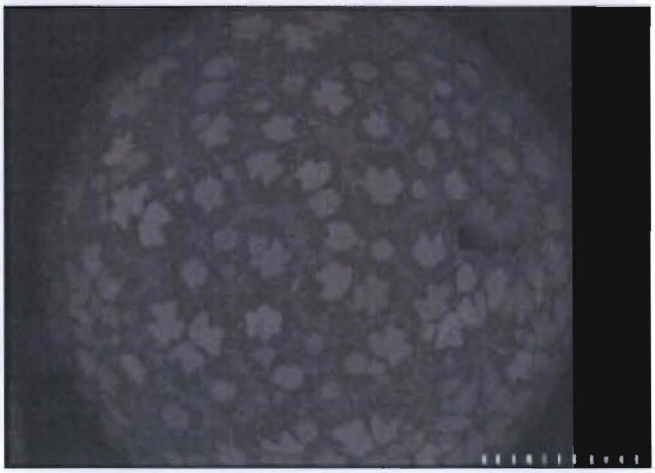

(b)

FIG. 8. Particle made from 75 Ce/25 Al evaporated until dry precusor. On the order of 10% of particles of this composition show this type of surface segregation. (a) Secondary electron image from the scanning electron microscope. (b) Backscatter image in which the light zones are ceria rich. The cerium rich zones correspond not simply to the light or dark areas on the backscatter image, but specifically to the darker areas (outlined) in the dark part of the secondary electron image. The particle is clearly hollow.

Figure 1 *Unique Structures*. Hollow ceramic Ce-Al oxide particles with surface segregation formed from ceria and alumina salts [58].

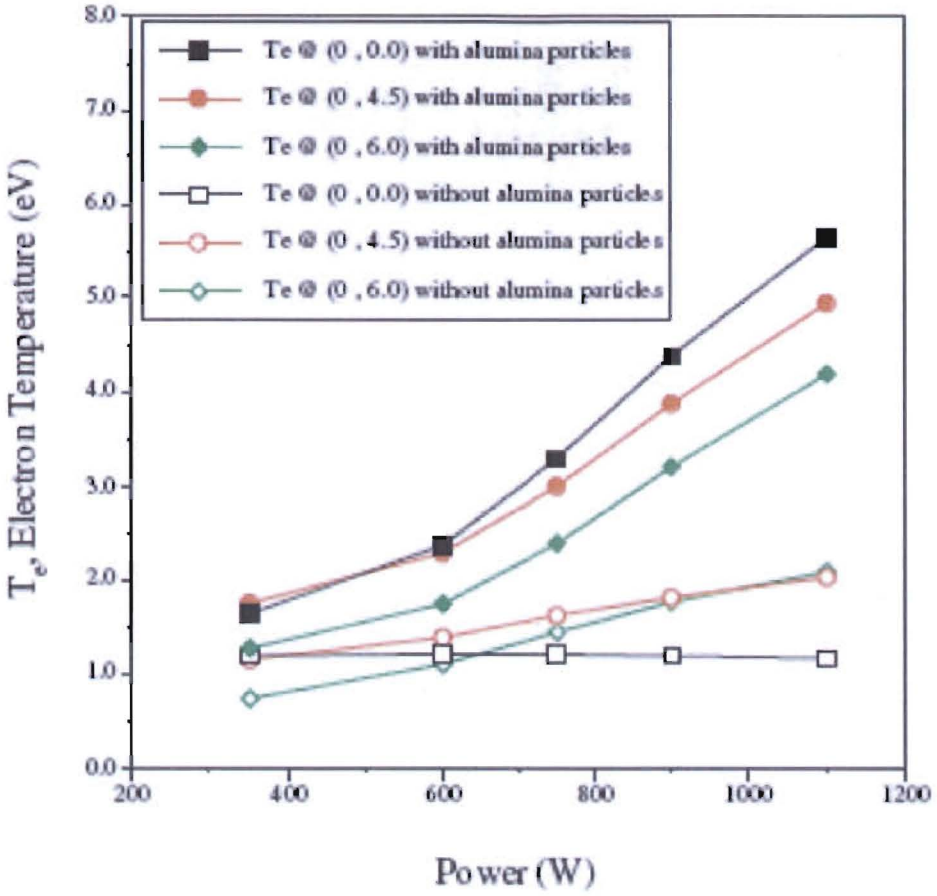

Figure 8. Electron temperature measured along the centre x-axis (with and without alumina particle) as a function of applied microwave power, x and z in mm. Experimental condition: plasma gas—1.171 min^{-1}, aerosol gas—0.361 min^{-1}, probe (H_2)—0.00051 min^{-1}. Note that with aerosol particles present the electron temperature is always significantly higher.

8

Fig. 12: *Charged Species Temperature Profile*. The temperatures are far higher in the presence of aerosol particles than they are in the absence of particles [91].

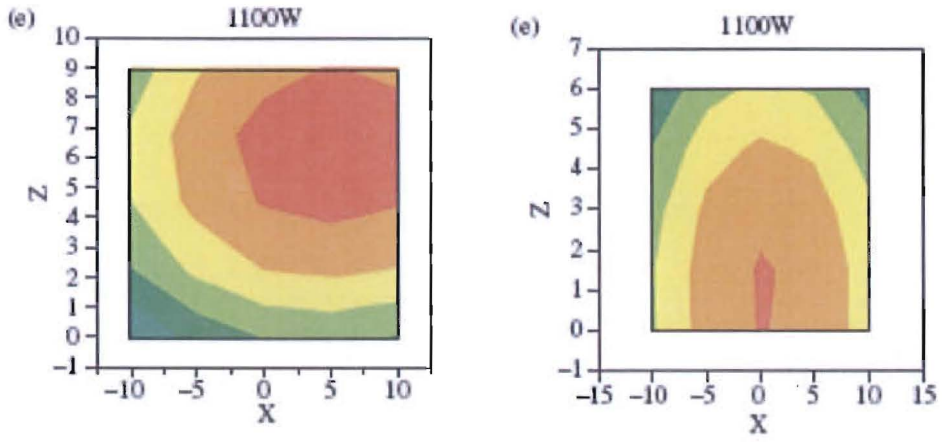

FIGURE 18: Charged Species Temperature Profile in Afterglow. Maps of the charged species temperature profiles, as a function of position in the afterglow, are shown. LEFT- In the absence of particles the highest temperature is found far above the top of the coupler. RIGHT- In the presence of a small volume (<1%) of micron alumina particles the maximum temperature is 3X larger than in the absence of particles, and the highest temperature, consistent with intuition, is directly above the coupler [91].